

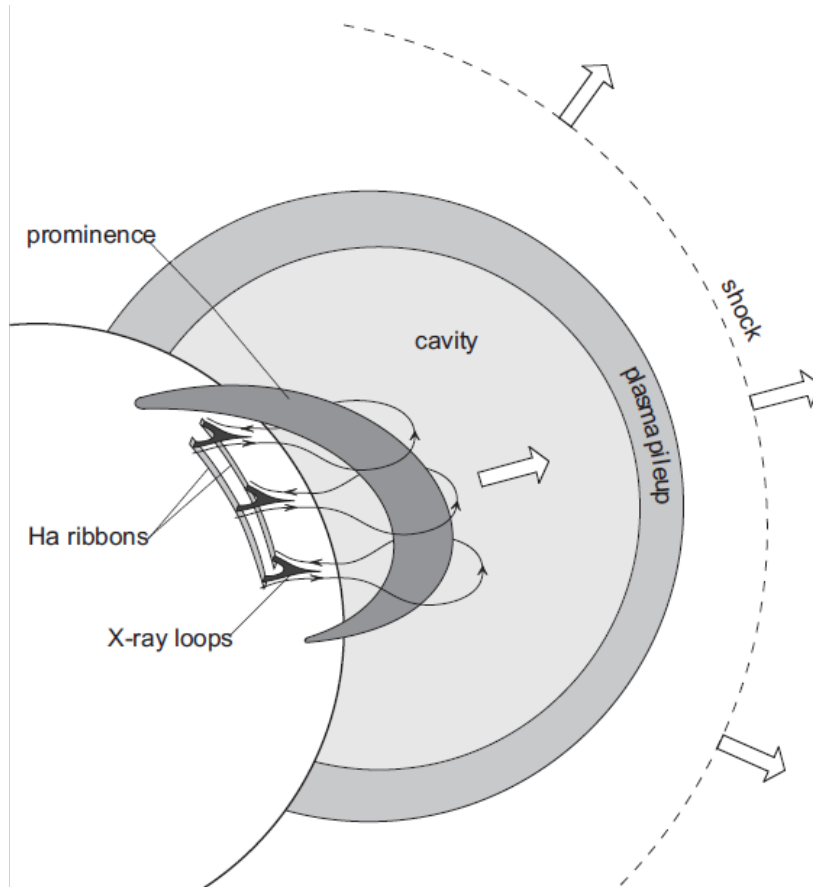
Dynamic evolution of coronal mass ejections

Manuela Temmer

Institute of Physics, University of Graz, Austria



Evolution of CMEs



Forbes 2000

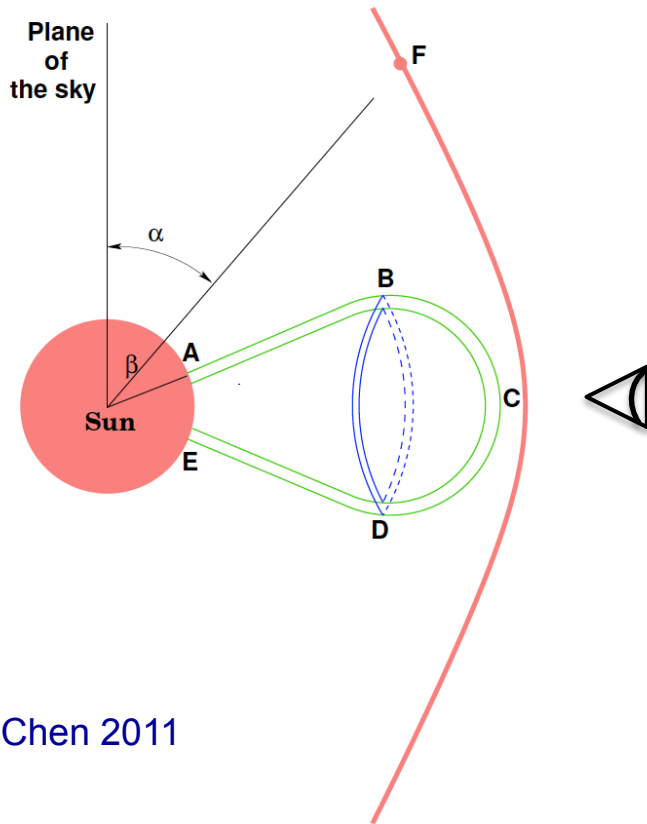
CMEs arise from closed magnetic field lines that begin as stable structures anchored to the Sun. Due to some instability the equilibrium is disrupted causing the eruption of the system (see e.g., [Forbes 2000](#))

Eruption due to magnetic reconnection or simple field reconfiguration ('stealth' CMEs, e.g., [Robbrecht et al., 2009](#))

CME front formed due to plasma-pileup / shock compression of plasma / or successive stretching of magnetic field lines (see review e.g., [Chen 2011](#))

2-front morphology (see [Vourlidas et al., 2013](#))

What do we actually observe?



Chen 2011

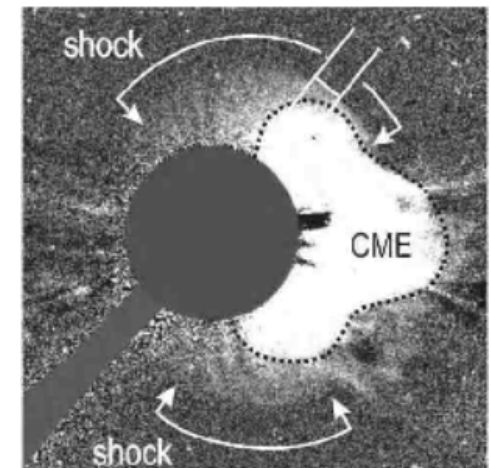
CME speeds, widths, locations measured from single v/p are projections on the plane-of-sky (e.g., [Hundhausen, 1993](#))

All derived parameters are severely affected by projection effects (see e.g., [Burkepile et al., 2004](#); [Cremades and Bothmer, 2004](#))

CME WL observations mostly mean to observe the shock-sheath structure due to shock compression (see e.g., [Ontiveros and Vourlidis, 2009](#))

Q: Are halo CMEs different from limb CMEs ([Chen, 2011](#))?

A: Halo CMEs do not show the actual size of a CME but the fast ms-shock wave ([Kwon et al., 2015](#))



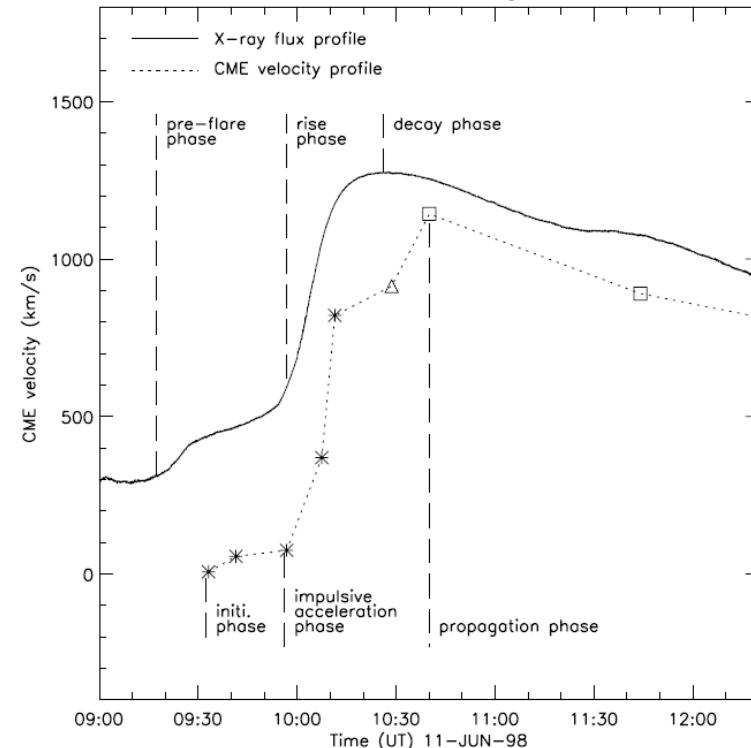
Ontiveros and Vourlidis, 2009

Kinematic properties of CMEs

Evolution of CMEs can be divided into three-phase scenario:
(Zhang et al., 2001; 2004; Chen and Krall, 2003)

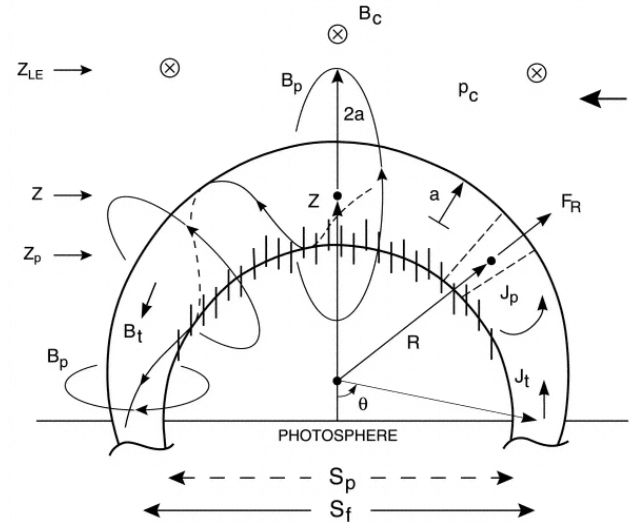
- Initiation of slow rising motion (some tens of minutes)
 - Non-coronagraphic/Coronagraphic FoV
- Impulsive or major acceleration phase where the maximum of acceleration and velocity is reached
 - Coronagraphic FoV/Heliospheric imagers
- Propagation phase during which the CME is adjusted to the speed of the ambient solar medium

Zhang et al., 2001



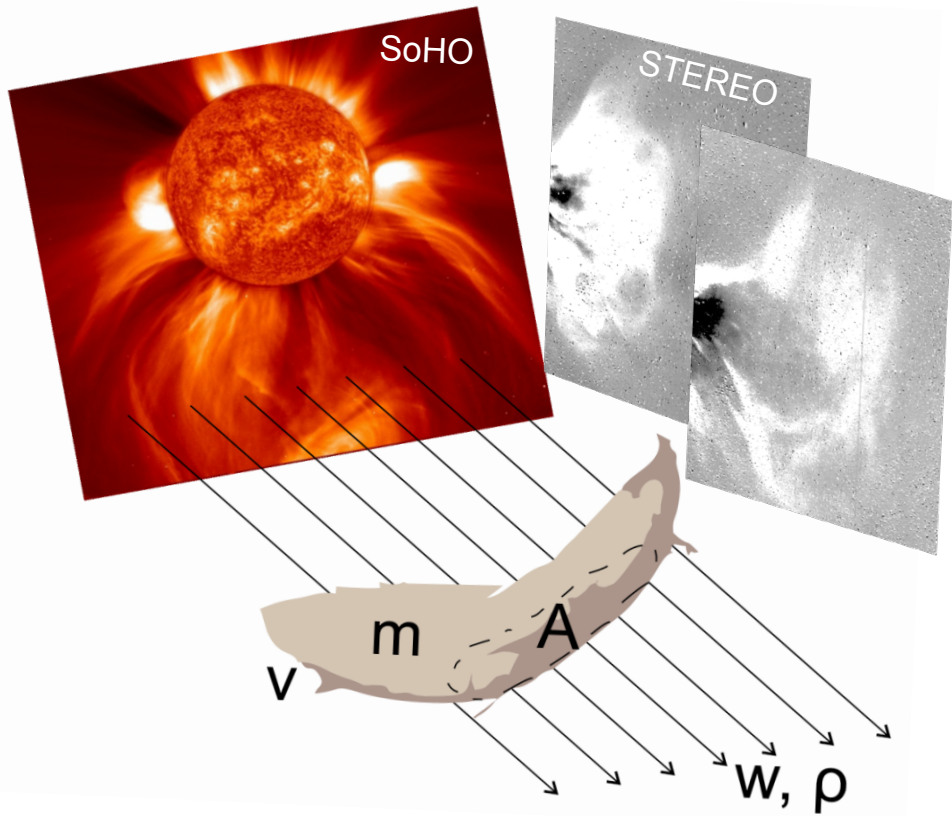
CME dynamics: Lorentz vs. drag force

Close to the Sun propelling *Lorentz force* as consequence of magnetic reconnection (e.g. [Chen 1989,1996](#); [Kliem & Török 2006](#))



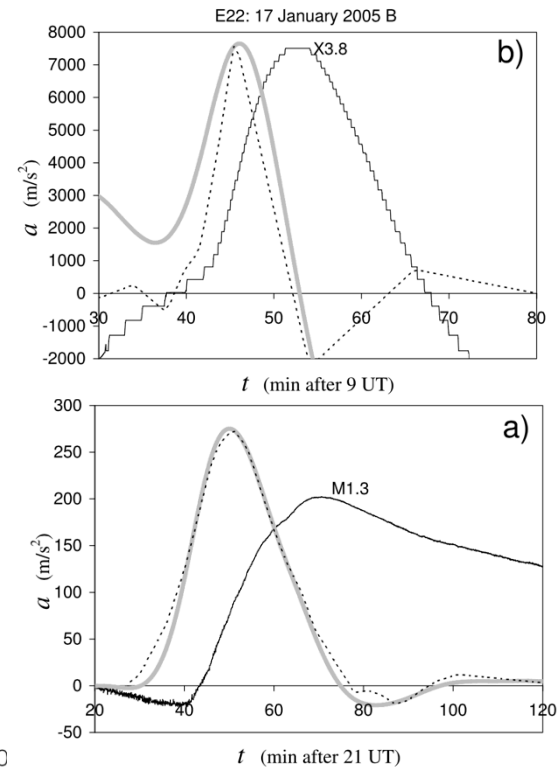
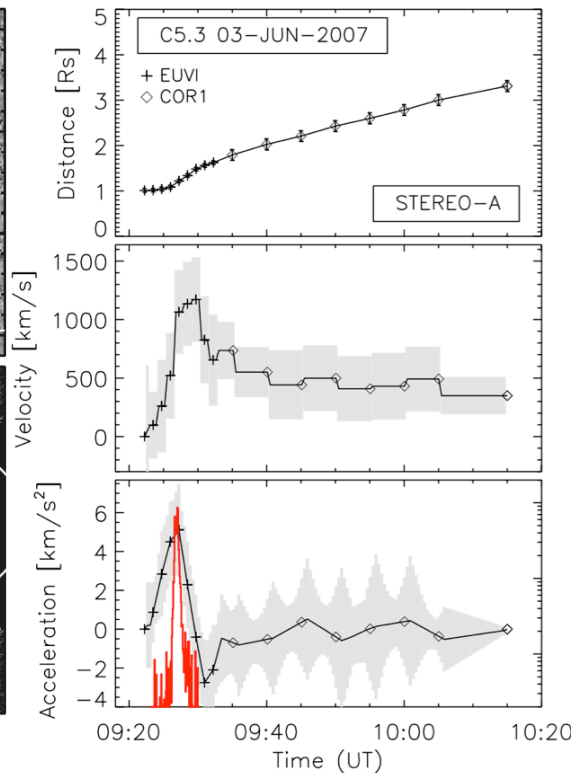
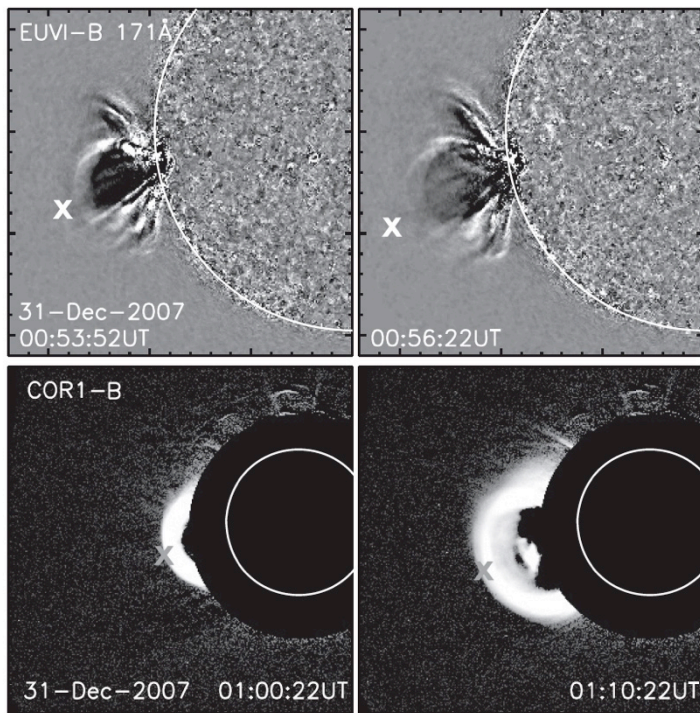
$$F = F_L + F_G + F_D$$

In IP space *drag* acceleration owing to the ambient solar wind flow (e.g. [Cargill et al. 1996](#); [Chen, 1996](#); [Cargill 2004](#); [Vršnak et al. 2004; 2013](#); [Maloney and Gallagher 2010](#), [Carley et al., 2012](#)).



Impulsive acceleration phase

- Detailed h - t profiles enable to study the impulsive acceleration phase with max. very low in the corona $<0.5R_s$ (Gallagher et al., 2003; Zhang and Dere, 2006; Vršnak et al., 2007; Bein et al., 2011)
- Flare-CME feedback relation (Maričić et al., 2007; Temmer et al., 2008; 2010; Chen and Kunkel, 2010; Berkebile-Stoiser et al., 2012)

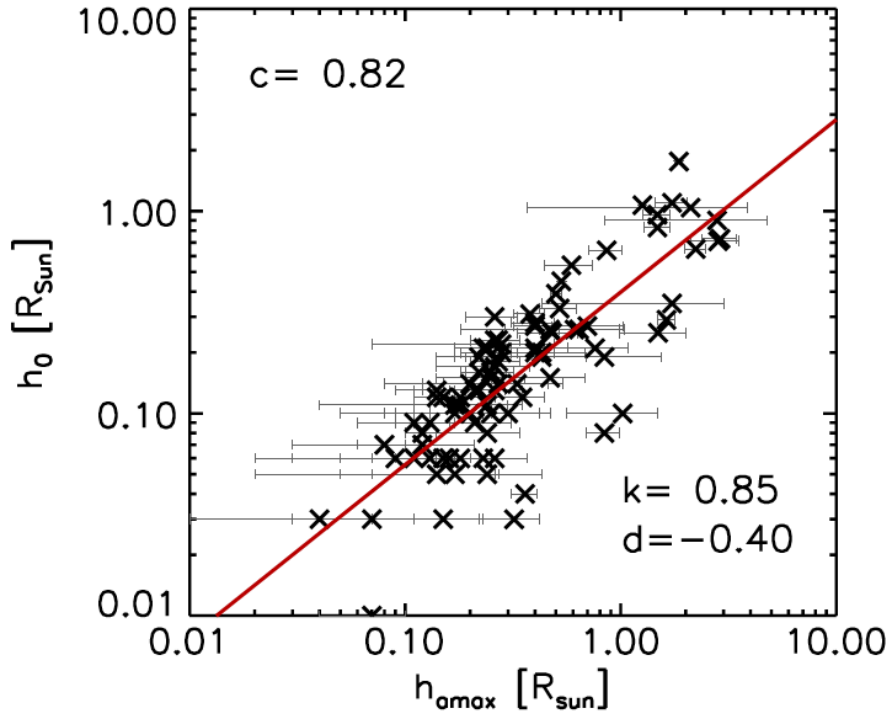


Temmer et al. (2010)

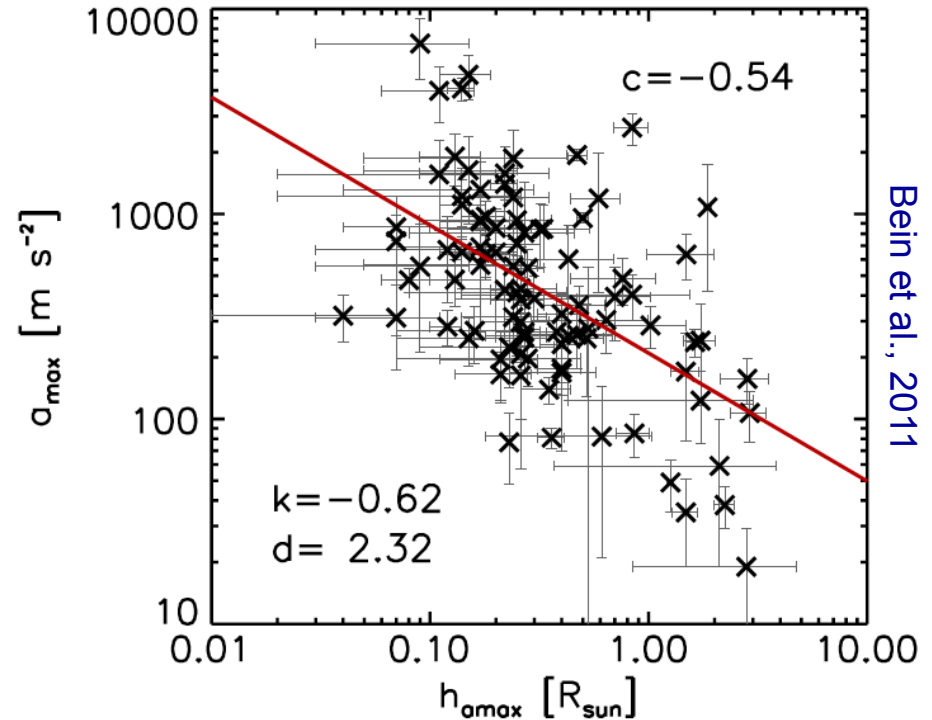
Maričić et al., 2007

CME properties are set in low corona

CMEs that start at lower heights also reach their peak acceleration at lower heights.



CMEs that are accelerated at lower heights reach higher peak accelerations.



Bein et al., 2011

The acceleration phase duration is proportional to the source region dimensions (compact CMEs are accelerated more impulsively; [Vrsnak et al., 2007](#)).

→ a consequence of stronger Lorentz force and shorter Alfvén time scales involved in compact CMEs (with stronger magnetic field and larger Alfvén speed being involved at lower coronal heights).

CME mass and energy – low corona

Projection effects - errors of factor 2 at 50-60° from from POS (Vourlidas et al., 2000)

3D/total mass: use two (or three) different vantage points (Colaninno and Vourlidas, 2009)

3D parameters for mass evolution:

$m_0 = 10^{14}g - 10^{16}g$ ($r < 3R_s$; initial mass)

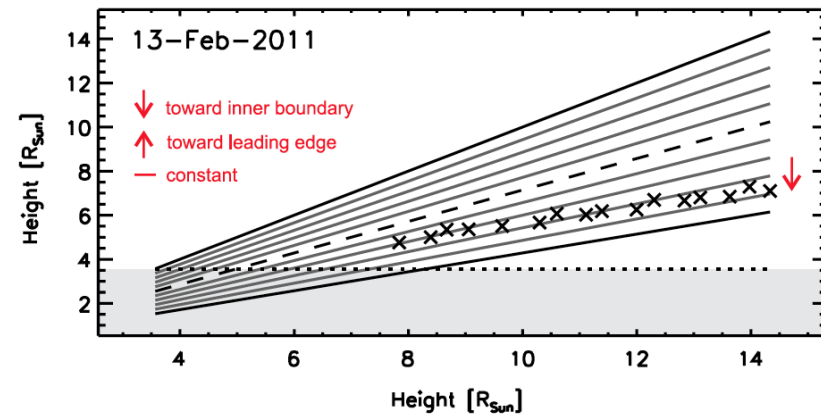
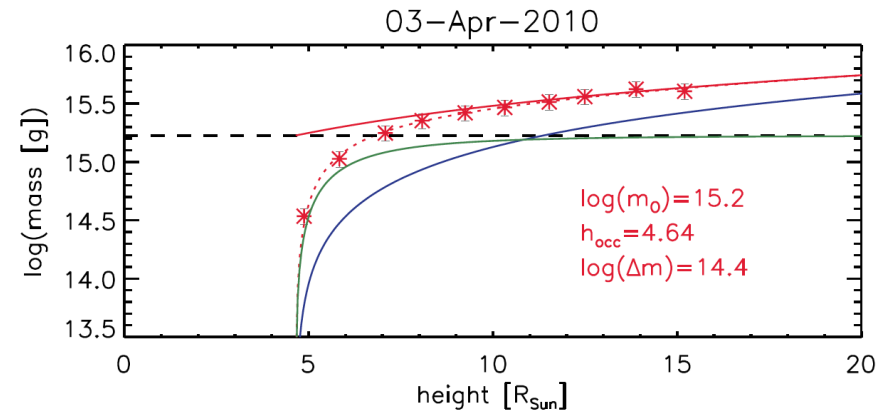
$\Delta m(r)$ mit $r=10-20R_s$: 2%-6%

Kinetic energy: $10^{23}J - 10^{25}J$

(see Bein et al., 2013)

$$m(h) = m_0 \left(1 - \left(\frac{h_{occ}}{h} \right)^3 \right) + \Delta m(h - h_{occ})$$

Bein et al., 2013



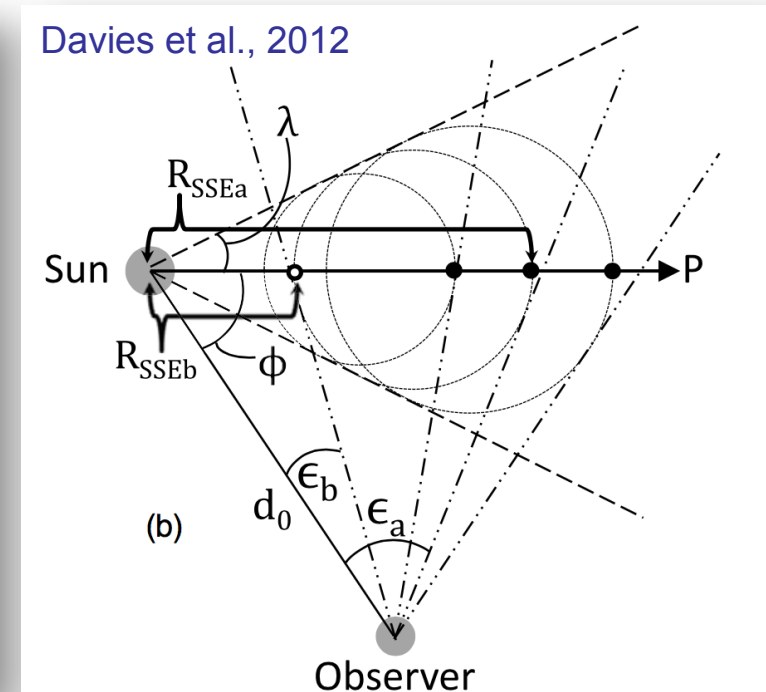
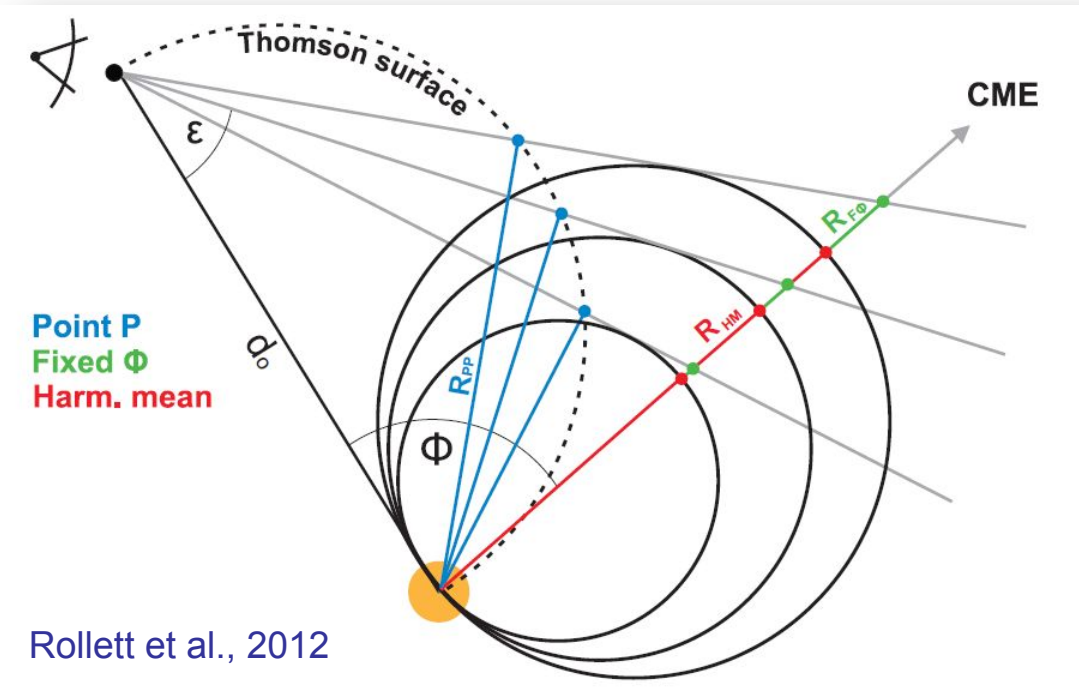
Important for studies on global energetics of flares and CMEs (see e.g., Emslie et al., 2004, 2012)

CMEs in IP space: elongation and geometry

Fixed- Φ (Sheeley et al., 1999; Kahler & Webb, 2007; Rouillard et al., 2008)

Harmonic Mean (Lugaz et al., 2009; Howard and Tappin, 2009)

Self Similar Expansion (Davies et al., 2012; Möstl and Davies, 2012; Möstl et al., 2015)



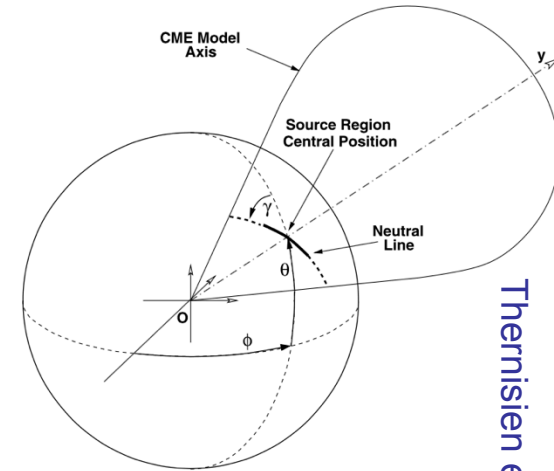
Remote sensing+in-situ:

Constrained Harmonic Mean (Rollett et al., 2012; Rollett et al., 2013)

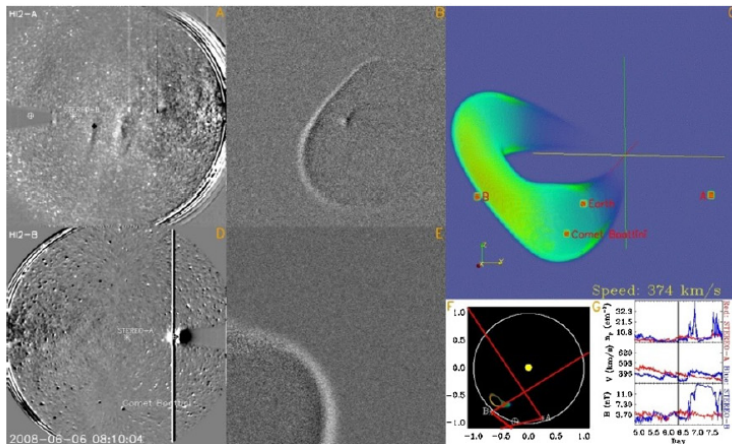
Constrained Self Similar Expansion (Rollett et al., 2014)

CME propagation direction (2 s/c)

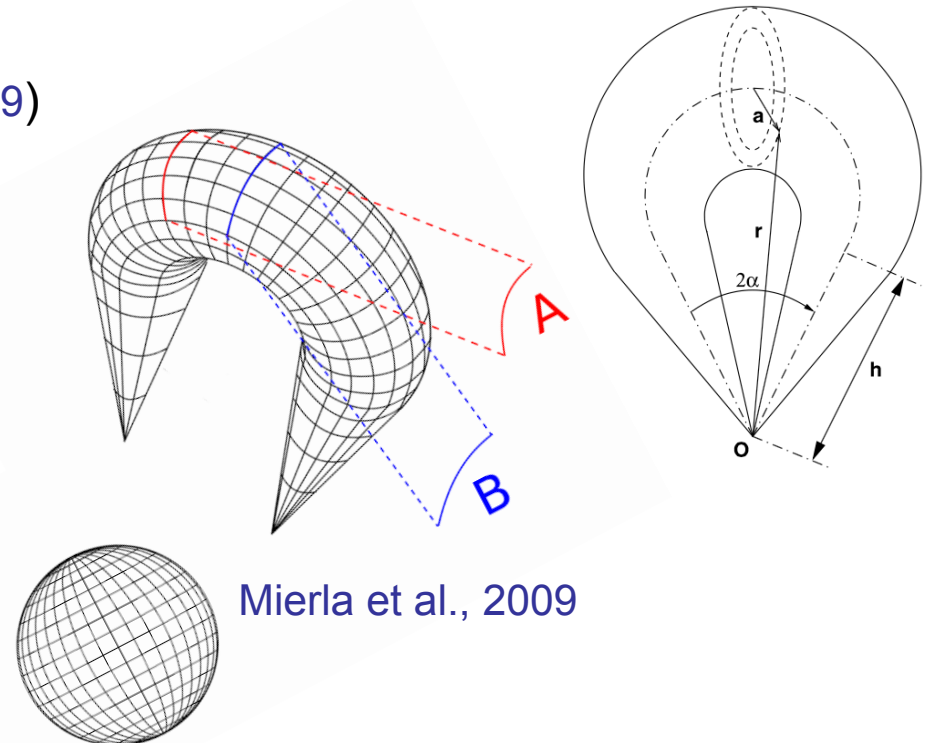
- Tie-point reconstruction, triangulation (e.g., Liu et al., 2009; Maloney et al., 2009; Mierla et al., 2009; Temmer et al. 2009; Byrne et al., 2010; Liu et al., 2010)
- Forward fitting of a model to white light images (Thernisien et al., 2006; 2009; Wood et al., 2009)
- CME mass calculation (Colannino and Vourlidas, 2009; Bein et al., 2013)
- Polarization ratio techniques (Moran et al., 2009; deKoning et al., 2009)



Thernisien et al., 2006



Wood et al., 2009



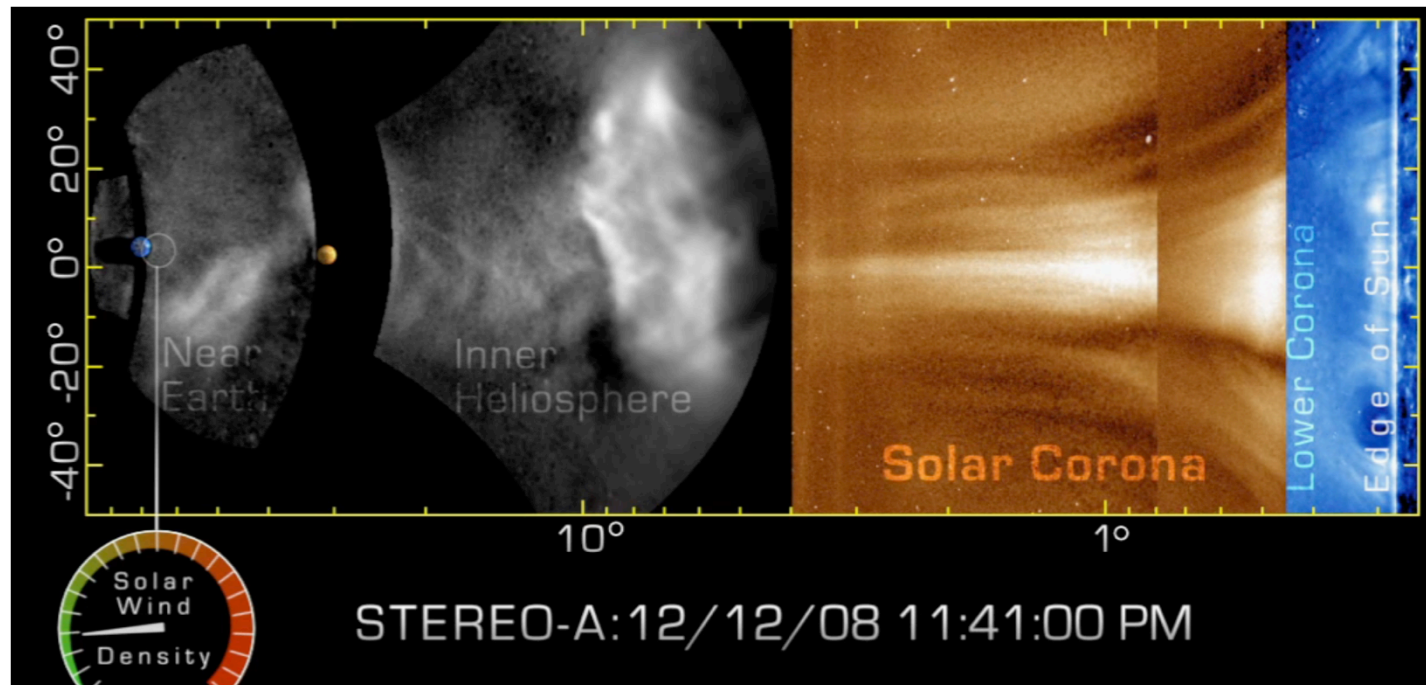
Mierla et al., 2009

Environmental conditions

Rotation of CMEs and adjustment to ambient magnetic field structure (see e.g., Yurchyshyn et al., 2001; 2009; Vourlidas et al., 2011; Isavnin et al., 2014)

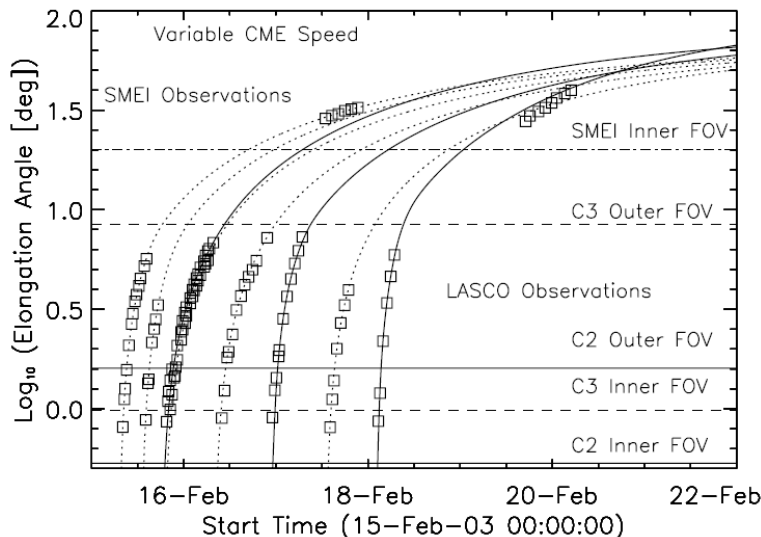
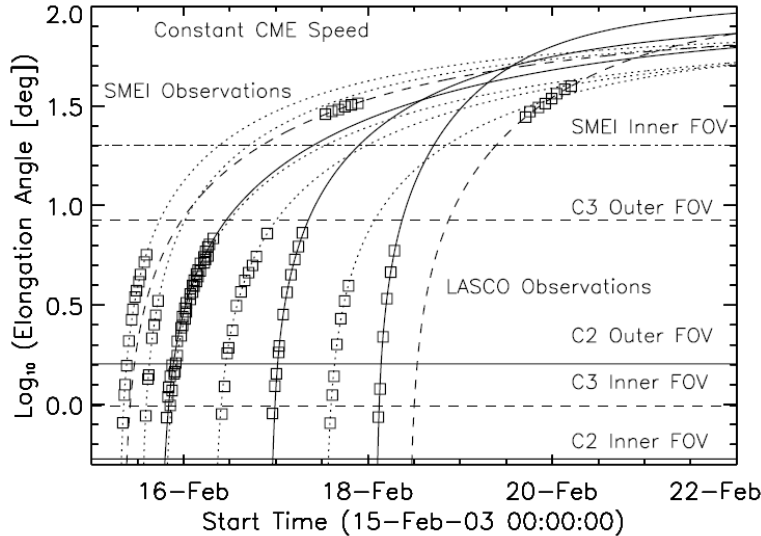
Latitudinal/Longitudinal deflection/channeling (e.g., MacQueen et al., 1986; Burkepile et al., 1999; Byrne et al., 2010; Foullon et al., 2011; Bosman et al., 2012; Wang et al., 2014; Möstl et al., 2015)

CME propagation/shape affected by interaction with the ambient SW (e.g., Manchester et al., 2004; Savani et al., 2010, Temmer et al., 2011; Rollett et al., 2014).



SWR, C.deForest

Effects of solar wind drag



- Constant speed fits do not match near-Sun and IP space observations simultaneously
- Empirical relation by Gopalswamy et al., 2001
 $a = -0.0054 (v - 406)$
- Observations using LASCO, SMEI, SECCHI data show drag effects (e.g., Tappin 2006; Howard et al., 2007; Morrill et al., 2009, Webb et al., 2009; Davis et al., 2010)
- Drag term is required (see also Howard et al., 2007; Webb et al., 2009)
- Solar minimum events: $v \sim const.$

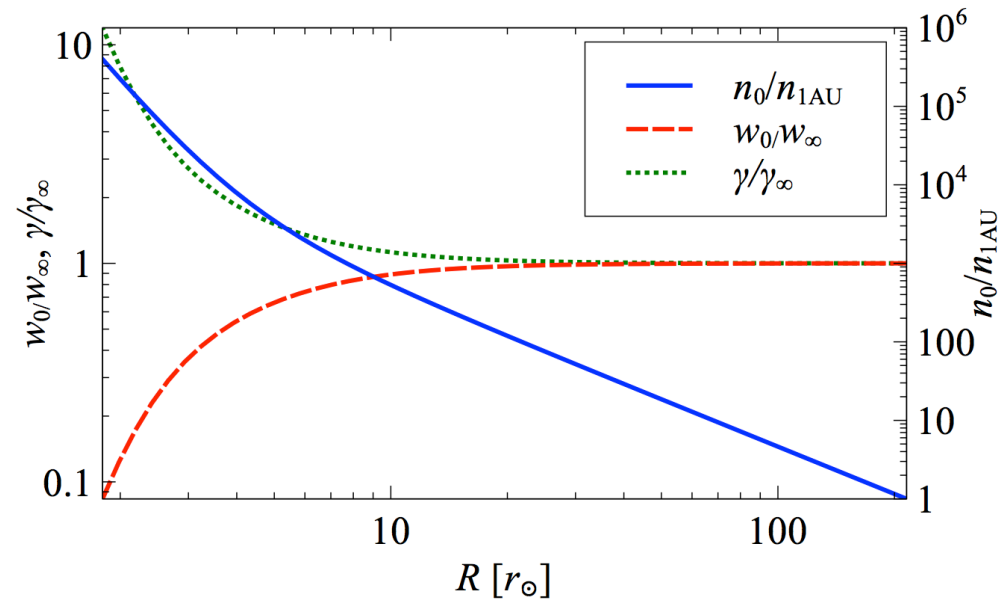
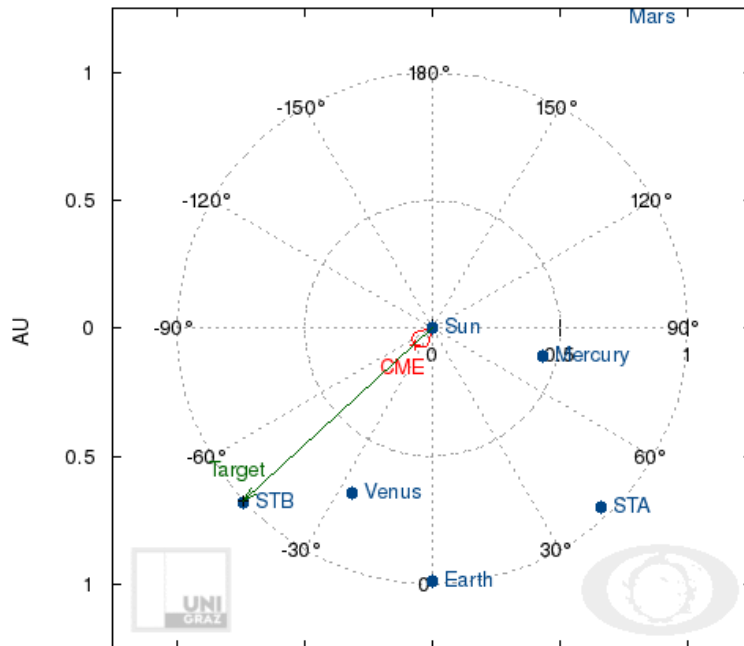
To fully understand the CME propagation behavior in IP space we need to know the spatial distribution of SW parameters.

Drag Based Model (DBM; Vršnak & Žic, 2007; Vršnak et al., 2013)

$$\frac{d^2r}{dt^2} = -\gamma(r) \left(\frac{dr}{dt} - w(r) \right) \left| \frac{dr}{dt} - w(r) \right| \quad \text{with} \quad \gamma = \frac{c_d A \rho_w}{V(\rho + \frac{\rho_w}{2})} = \frac{c_d}{L(\frac{\rho}{\rho_w} + \frac{1}{2})}$$

$$w(R) = \begin{cases} w_0(R) + w_p(R), & R_1 < R < R_2 \\ w_0(R), & \text{otherwise} \end{cases}$$

Disturbed solar wind e.g., CME-CME interaction, HSS interaction (Žic et al., 2015).



<http://oh.geof.unizg.hr/DBM/dbm.php>

Forecasting CME arrival times

*On a statistical basis, accuracy of forecasting CME arrival times: $\pm 8-12$ hrs.
Prediction accuracy degrades with increasing activity (preconditioning).*

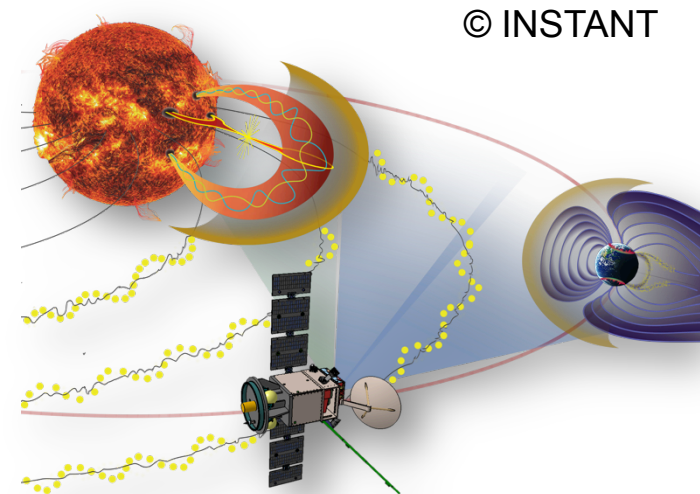
Linear fit for $r > 50R_s$ matches best w/ arrival times: ± 6 hrs for 80% of events; $\Delta v = \pm 140$ km/s (Colaninno et al., 2013).

Average absolute error in ENLIL realtime forecasts is $\pm(7.5-12)$ hrs (Romano et al., 2013).

DBM-ENLIL comparison for real-time forecasted events, $\Delta t \sim 7$ hrs. O – C: -0.3 ± 17 hrs for ENLIL / -1.7 ± 18.3 hrs for DBM (Vršnak et al., 2014).

Absolute difference O – C = 8.1 ± 6.3 hrs for CMEs tracked up to $30-50^\circ$ elong.; $\Delta v = 284 \pm 288$ km/s (Möstl et al., 2014).

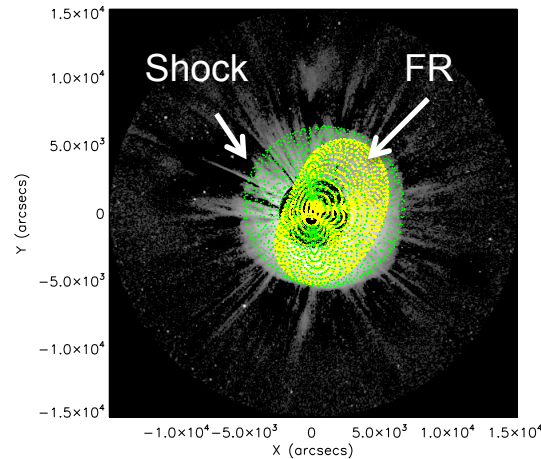
Combined GCS 3D and drag force model: ± 6.8 hrs to ± 12.9 hrs (Shi et al., 2015).



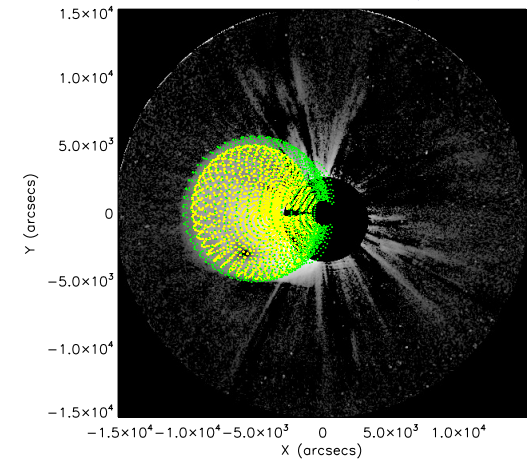
*Support of instruments
away from Sun-Earth line!*

July 23, 2012: the super-fast CME

- Less than 21 hours (Sun-1AU)
- ST-A in-situ speed 2250 km/s;
ICME1: complex; 110nT,
ICME2: cloud-like; 50nT;
(cf. [Russell et al., 2013](#))



Temmer and Nitta, 2015



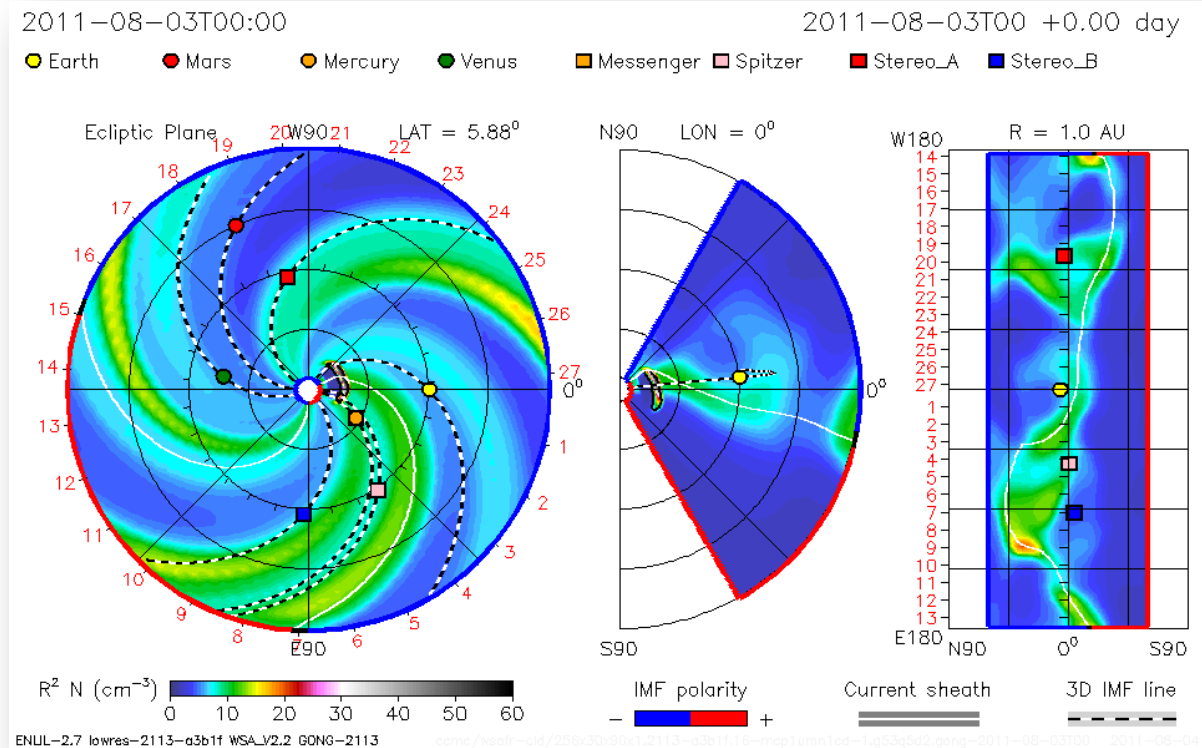
- If Earth-directed: high speed and magnetic field (neg. Bz) might have caused an extreme Space Weather event; Dst of -600 to -1100 nT (e.g., [Ngwira et al., 2013](#); [Baker et al., 2013](#); [Liu et al., 2014](#))
- [Liu et al., 2014](#): CME-CME interaction event which produced complex and high magnetic field (due to compression); **preconditioning** of IP space due to an earlier fast CME event from July 19, 2012
- [Temmer and Nitta, 2015](#): Complex two-stage eruption; extremely powerful acceleration (CME was driven over a period of about 1 hour and up to 10Rs); extreme low drag effect due to low ambient density ($\gamma = 0.01$)

Preconditioning: CME – CME interaction

CME occurrence rate: 0.3 per day (solar min) to 4-5 per day (solar max)
(e.g., St. Cyr et al., 2000, Gopalswamy et al., 2006).

CME transit time from Sun to 1AU: 1 to 4 days (average speed: 500 km/s
with maximum speeds up to 3000 km/s).

During times of high solar activity, CME-CME interaction is assumed to happen frequently.

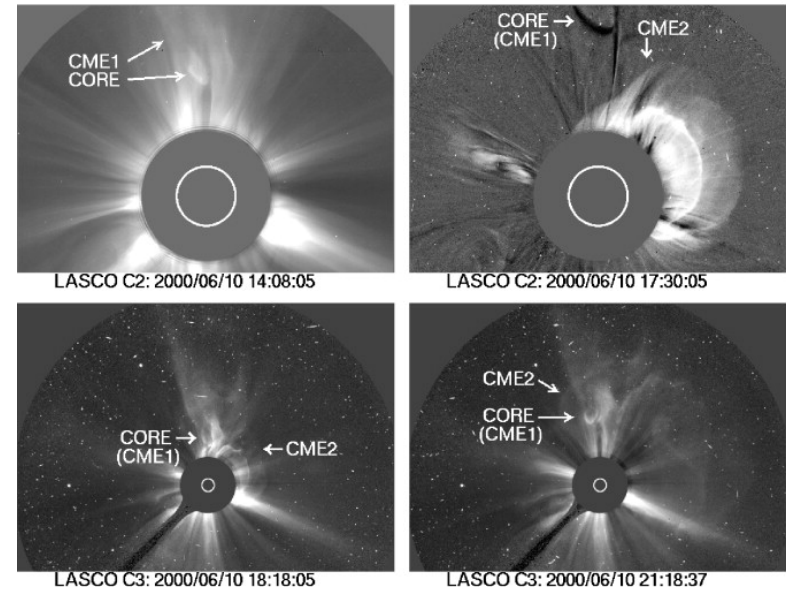


CME – CME interaction

Successive CMEs (**similar directions**) may merge and form complex ejecta of single fronts (e.g., Gopalswamy et al. 2001; Burlaga et al. 2002, 2003; Wang et al. 2002; Wu et al., 2007).

Radio enhancements, SEPs – acceleration at shock front or from regions with access to solar wind magnetic field lines? (e.g., Gopalswamy et al. 2001; 2002; Hillaris et al., 2011; Kahler & Vourlidas 2014)

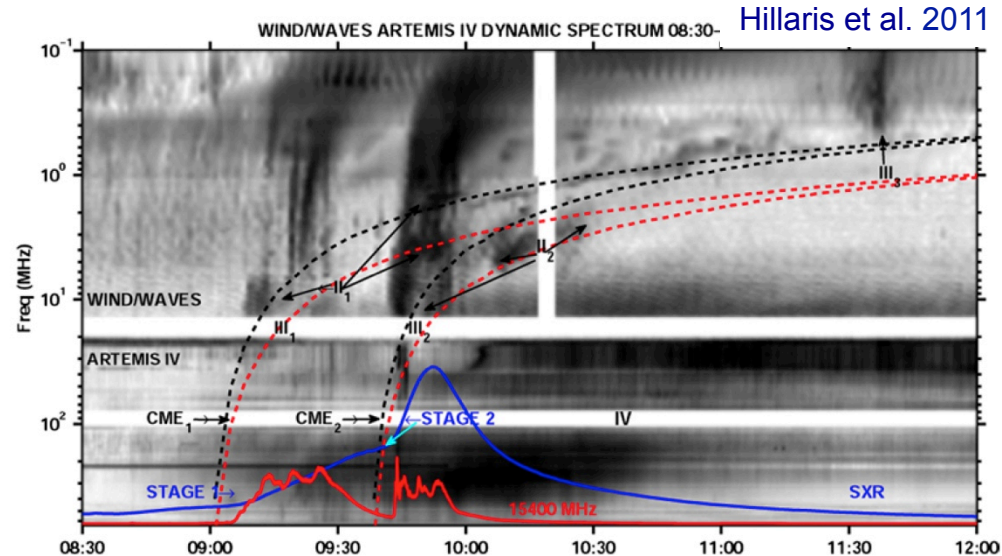
Gopalswamy et al. 2001



Effects at Earth:

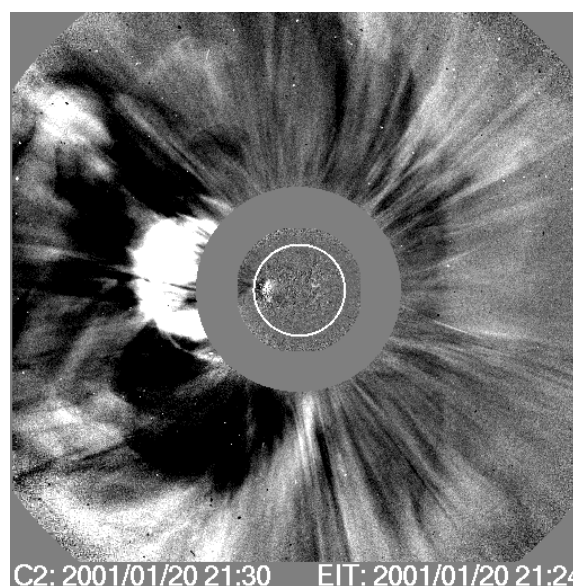
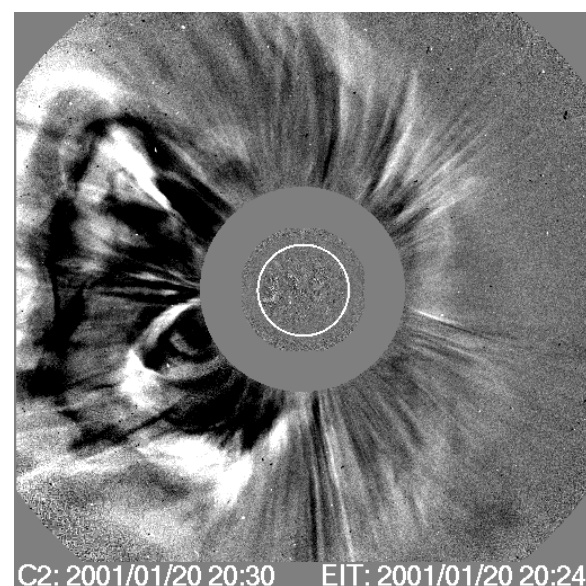
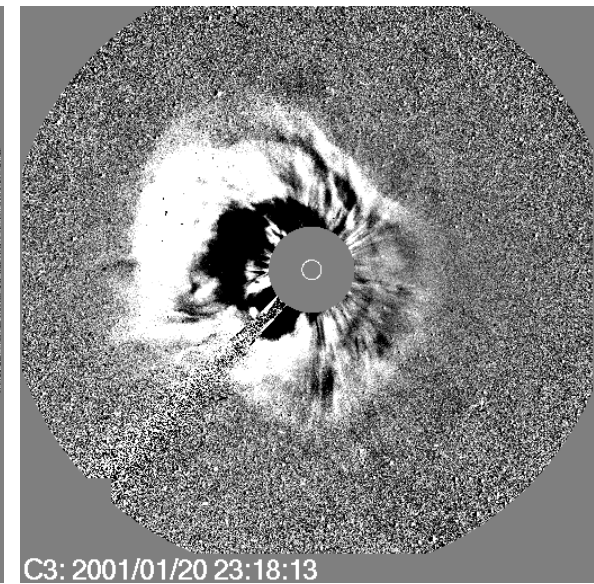
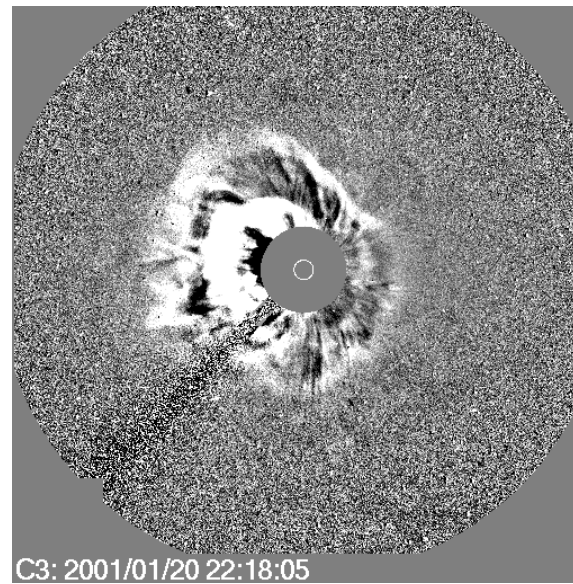
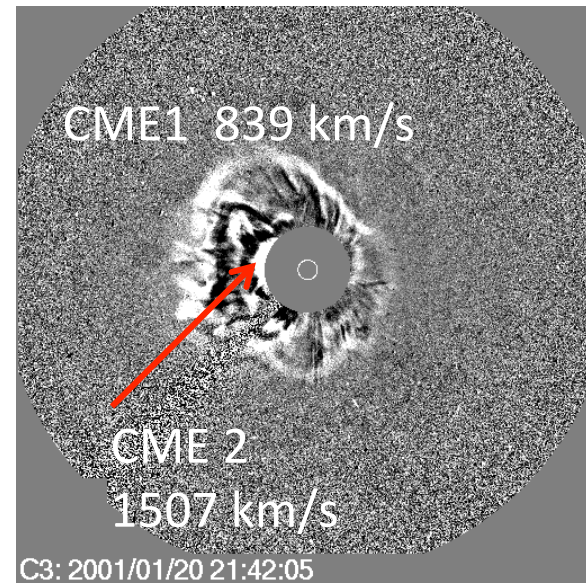
- extended periods of negative Bz (e.g. Wang et al. 2003; Farrugia et al. 2006)
- intense geomagnetic storms (Burlaga et al. 1987; Farrugia et al. 2006a,b; Xie et al. 2006)

Hillarlis et al. 2011



Cannibalism of CMEs?

Gopalswamy et al., 2001



Cannibalism, i.e. total reconnection?

Alfvén speed within structures is low, reducing efficiency of reconnection process (Bojan Vršnak, private communication)

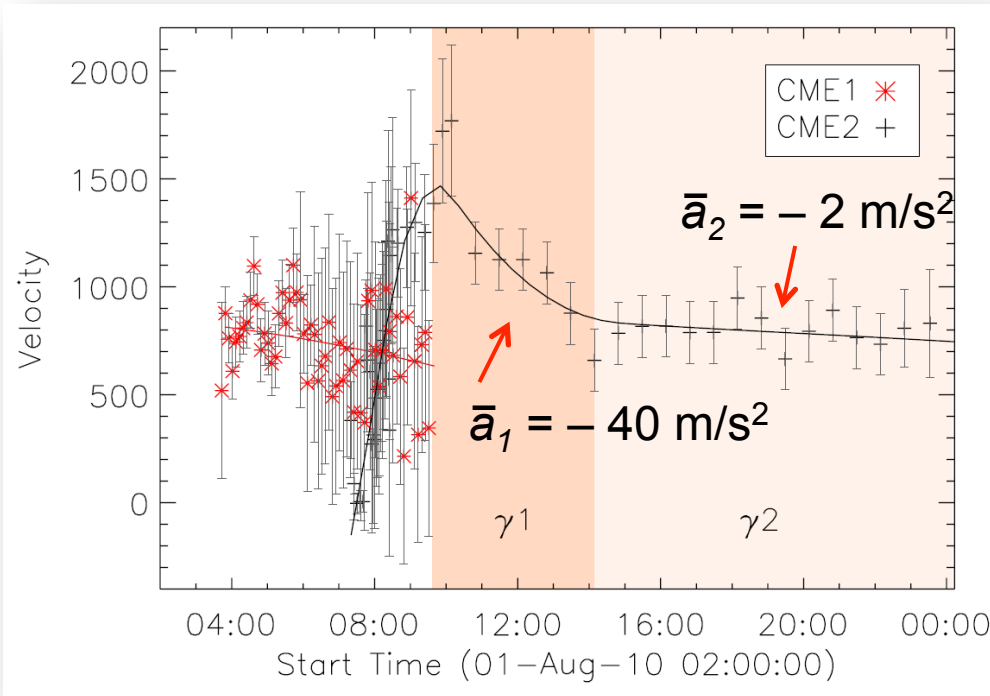
In-situ data – two FR? (Lugaz and Farrugia, 2014).

Observations of interaction

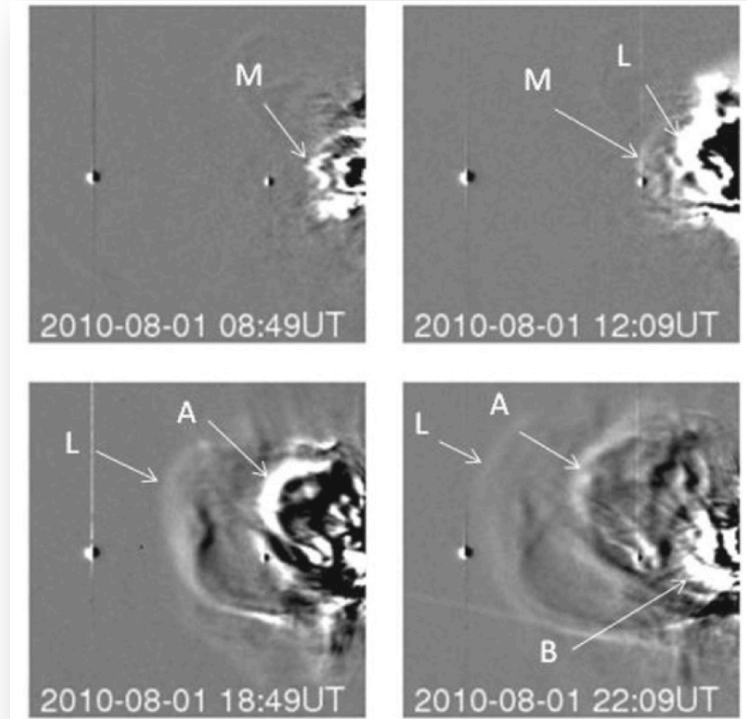
Strong deceleration hours before interaction of CME leading edges – transfer of momentum (see e.g., Farrugia & Berdichevsky, 2004; Maričić et al., 2014)



Temmer et al., 2012

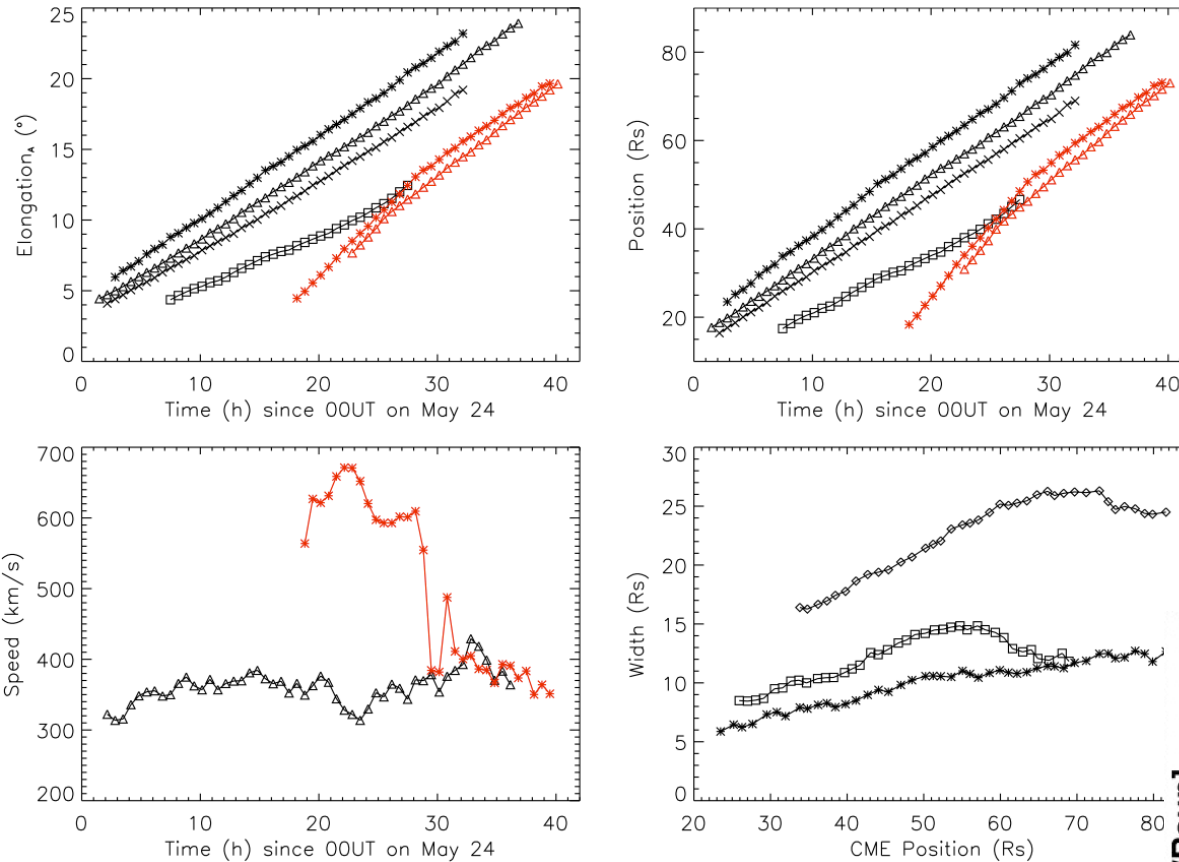


Harrison et al., 2012



Various aspects of August 1, 2010 events: Harrison et al., 2012; Liu et al., 2012; Martinez-Oliveros et al., 2012; Möstl et al., 2012; Temmer et al., 2012; Webb et al., 2012;

CME-CME interaction scenarios

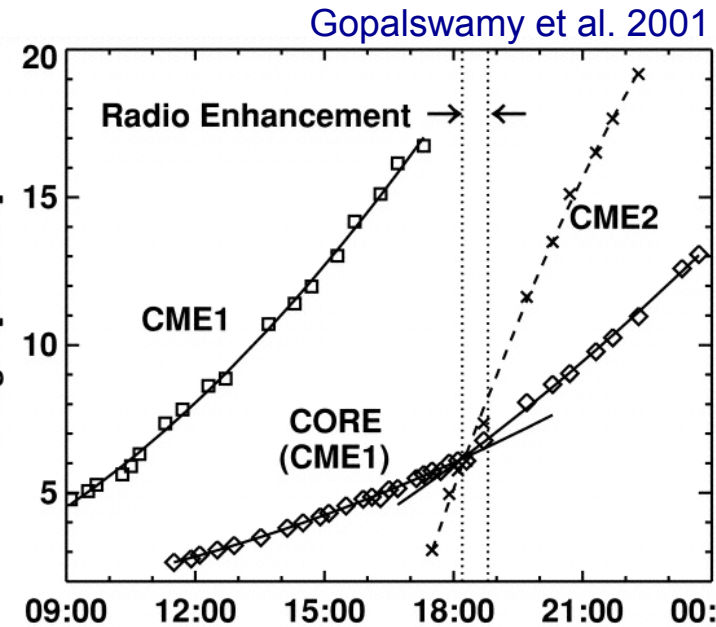


CME2 decelerates, CME1 slightly accelerates during collision ($m_{\text{CME1}} \sim m_{\text{CME2}}$).

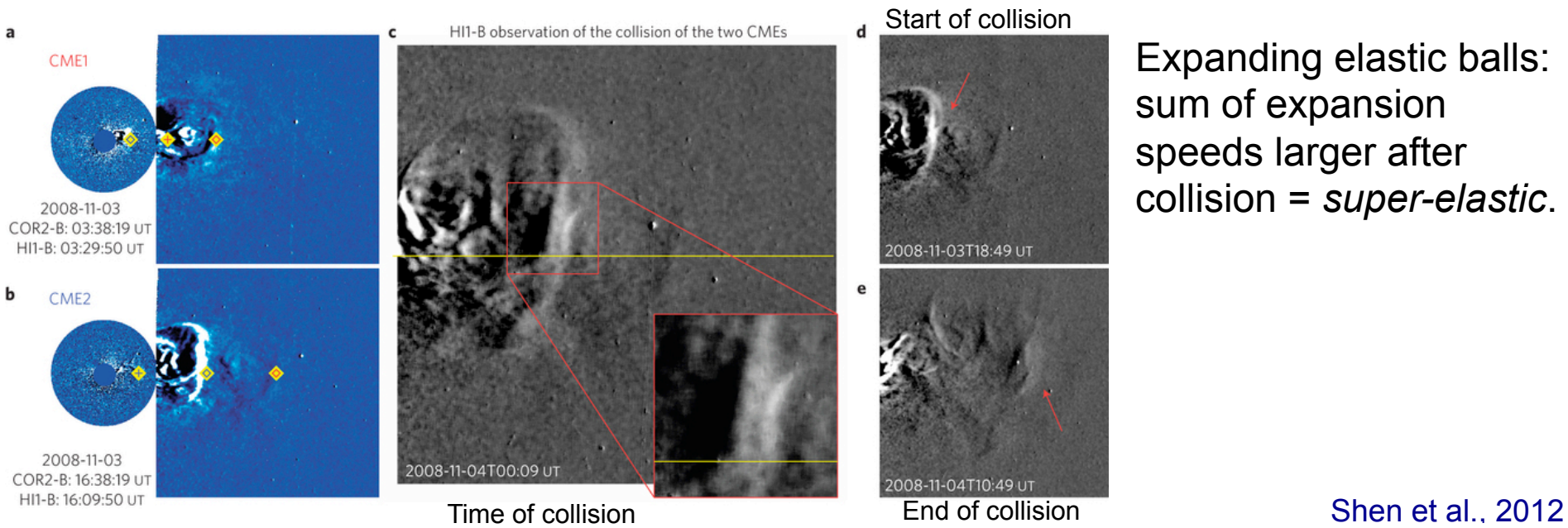
Perfectly inelastic collision (see also [Lugaz et al., 2009](#); [Mishra et al., 2014, 2015](#)).

[Lugaz et al., 2012](#)

Problems in determining the type of collision, such as changes in mass, direction, ... (e.g., [Liu et al., 2012](#); [Lugaz et al., 2013](#)).



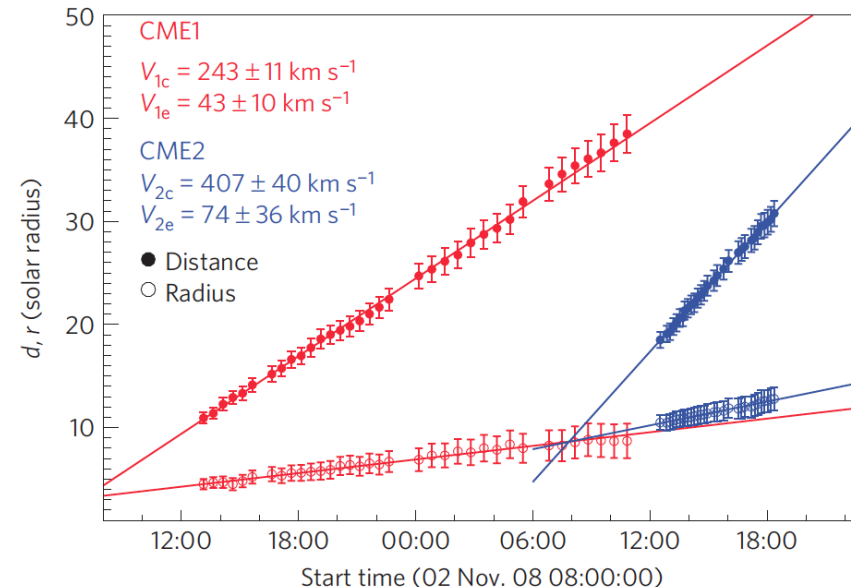
CME-CME interaction scenarios



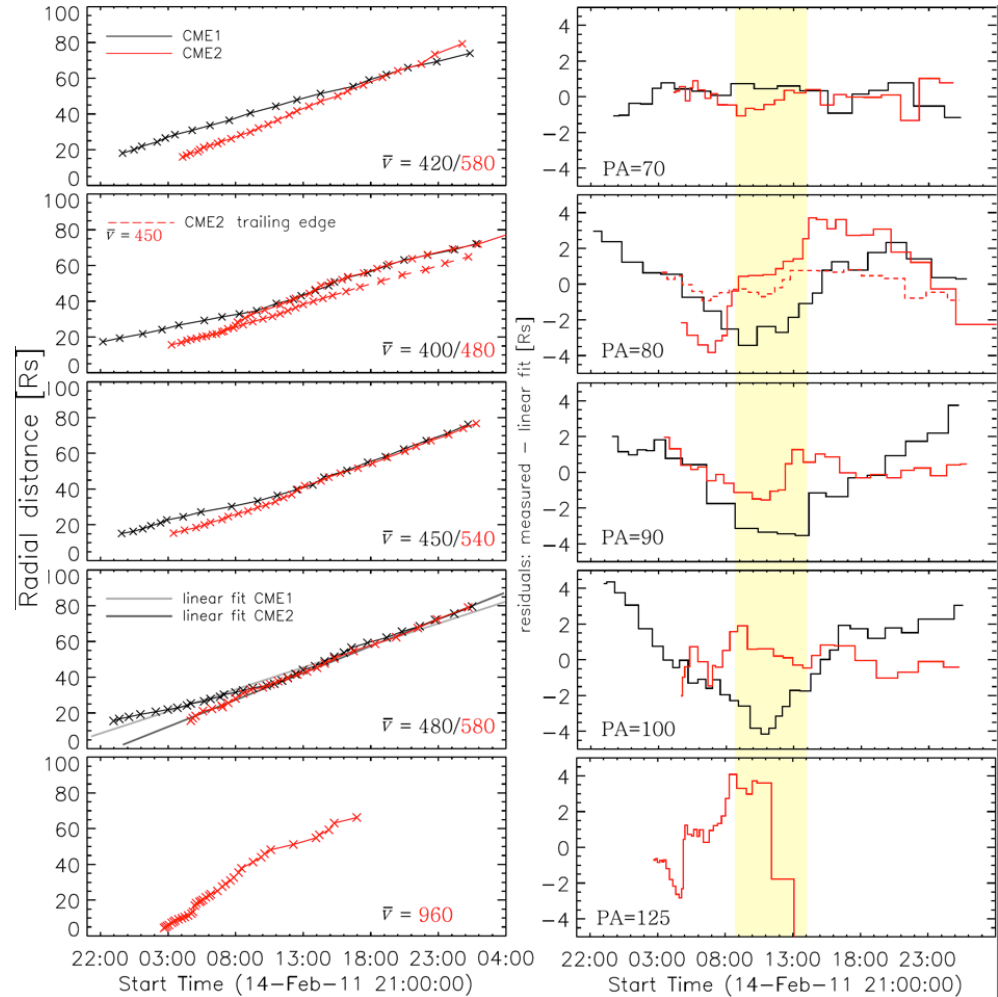
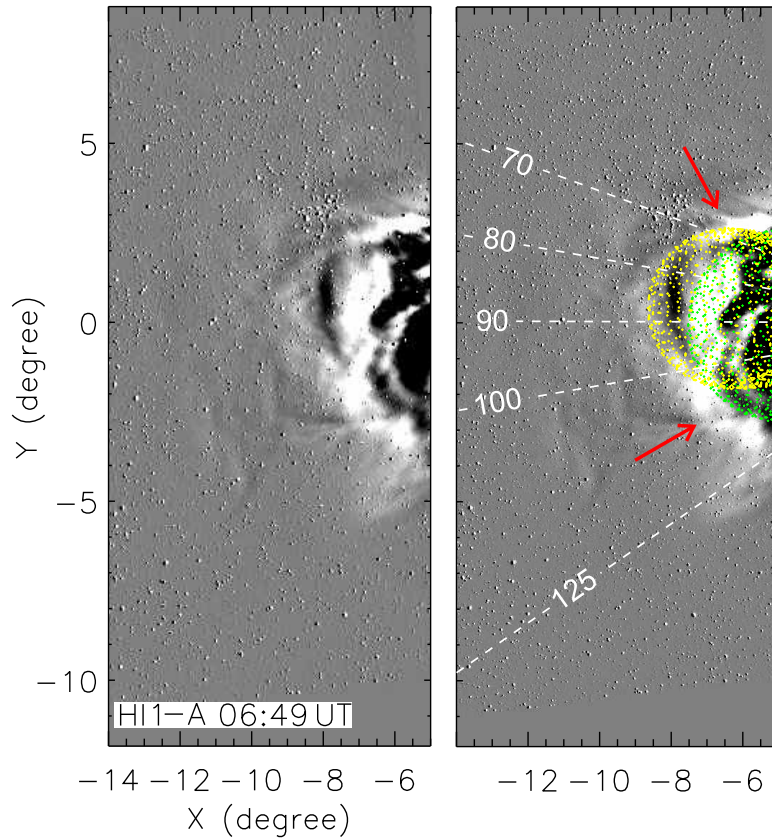
Shen et al., 2012

Conversion of magnetic and thermal energies into kinetic energy (cf. Shen et al., 2013).

In-situ data may give more hint on that – however, measurements are far from actual site of collision (future missions!).



Observations of interaction



Asymmetric interaction process
maybe related to FR location.

Observational data reveal only the consequences of CME–CME interaction that may not be sufficient to fully describe the process of interaction (Temmer et al., 2014).

Summary and conclusions

- CME properties are set in the low corona (source region characteristics, magnetic reconnection process which links flares and CMEs)
- Ambient magnetic field configuration controls changes in CME propagation behavior (strong overlying fields; magnetic pressure gradient)
- Propagation behavior of CMEs in IP space strongly affected by the characteristics of the ambient solar wind flow
- CME-CME interaction: extreme changes in CME dynamics; may happen quite often
- Preconditioning (density, B) may play an important role
- CME/Space Weather forecast: tools might need *permanent* update (implement EACH event!); event-based forecasts might not improve accuracy

